

# Preparation and Characterization of Cellulose Regenerated from Phosphoric Acid

Xuejuan Jia, Yingwen Chen, Chong Shi, Yangfan Ye, Peng Wang, Xiaoxiong Zeng, and Tao Wu\*

College of Food Science and Technology, Nanjing Agricultural University, Weigang 1, Nanjing 210095, People's Republic of China

**ABSTRACT:** Native cellulose has a highly crystalline structure stabilized by a strong intra- and intermolecular hydrogen-bond network. It is usually not considered as a good gelling material and emulsion stabilizer due to its insolubility in water. Chemical modification is generally necessary to obtain cellulose derivatives for these applications. In this study, we have shown that, by simply disrupting the hydrogen-bond network of cellulose with phosphoric acid treatment, the regenerated cellulose can be a good gelling material and emulsion stabilizer. Microscopy, X-ray diffraction, and Fourier transform infrared spectroscopy analysis have confirmed that the regenerated cellulose is primarily amorphous with low crystallinity in the structure of cellulose II. Stable aqueous suspensions and opaque gels that resist flowing can be obtained with the regenerated cellulose at concentrations higher than 0.6% and 1.6%, respectively. Moreover, it can effectively stabilize oil-in-water emulsions at concentrations less than 1% by a mechanism that combines network and Pickering stabilization.

**KEYWORDS:** phosphoric acid, regenerated cellulose, gel, emulsion stabilization, Pickering, network stabilization

## INTRODUCTION

Cellulose is the most abundant and renewable functional biopolymer created by nature; it exists in all higher plants, certain species of marine animals, bacteria, algae, and fungi.<sup>1</sup> Native cellulose has a highly crystalline structure stabilized by a strong intra- and intermolecular hydrogen-bond network.<sup>2</sup> It is usually not considered as a good gelling material and emulsion stabilizer due to its insolubility in water.<sup>3</sup> Chemical modification is generally necessary to obtain cellulose derivatives with improved water solubility for applications of gelling and emulsion stabilization, such as carboxymethylcelluloses (CMCs), methylcelluloses (MCs), and hydroxypropylmethylcelluloses (HPMCs).<sup>3</sup> Partial hydrolysis of purified wood pulp cellulose can obtain an insoluble cellulose material termed microcrystalline cellulose (MCC).<sup>4</sup> Blending of MCC with anionic polysaccharides such as sodium CMC, xanthan, or sodium alginate can obtain a colloidal form of MCC, which is water dispersible and can be used to stabilize foams and emulsions.<sup>4</sup>

Recently the gelling and emulsion stabilization properties have been explored in a new family of cellulosic materials—nanocelluloses.<sup>5–8</sup> The supramolecular structures of native cellulose have both amorphous and crystalline domains, in which the latter can be released by acid hydrolysis or mechanical treatments to produce various forms of nanocelluloses, such as nanocrystalline cellulose (NCC), microfibrillated cellulose (MFC), or nanofibrillated cellulose (NFC) depending on the preparation method and source.<sup>7</sup> By acid hydrolysis, the amorphous domain is hydrolyzed with hydrochloric acid or sulfuric acid, or, less frequently, with phosphoric acid, leaving the crystalline domain as NCC.<sup>9</sup> Due to the harsh reaction conditions used and the resulting acid degradation of the amorphous region, the yield of NCC is generally low and was reported to be approximately 30%, even after optimization of the reaction conditions.<sup>10</sup> By mechanical treatments, cellulose fibers are delaminated by high pressure homoge-

nization, microfluidizers, or sonication to produce MFC or NFC, usually after carboxymethylation or enzymatic pretreatment to decrease the adhesion between cellulose fibrils.<sup>11</sup> The energy consumption of the mechanical treatment is very high, reaching 25,000 kWh per ton in the preparation of MFC.<sup>7</sup>

The morphology of the cellulose nanocrystals is generally needle or rod shaped with widths of a few nanometers and lengths varying from tens of nanometers to several micrometers.<sup>2</sup> They typically have the same crystalline structure as their original fibers, although transformation from cellulose I to cellulose II was occasionally found.<sup>12</sup> If prepared by HCl hydrolysis, the surfaces are weakly negatively charged, as a result of the carboxylic groups in the residual hemicelluloses that were not removed during purification.<sup>13,14</sup> Due to the same reason, MFCs and NFCs are also weakly negatively charged. However, if prepared by H<sub>2</sub>SO<sub>4</sub> hydrolysis, there is a stronger negative charge due to the introduction of sulfate ester groups during the preparation.<sup>14</sup> Because of these charges, cellulose nanocrystals present good colloidal stability and dispersibility. NCCs prepared with HCl can be dispersed by the thorough removal of acid from the hydrolysate.<sup>14</sup> NFCs prepared after a carboxymethylation pretreatment are readily dispersed by sonication at neutral pH and under salt-free conditions.<sup>11</sup> NCCs prepared with H<sub>2</sub>SO<sub>4</sub> can be dispersed in aqueous solution with a pH ranging from 2 to 11.<sup>5</sup> If prepared with H<sub>3</sub>PO<sub>4</sub> hydrolysis, they are readily dispersible in polar solvents.<sup>9</sup> However, the colloidal stability of cellulose nanocrystals is sensitive to electrolytes due to specific interactions of counterions with the deprotonated carboxyl groups and the screening effect of the salt.<sup>5</sup> Nanocelluloses are excellent gelling materials, and their gelling properties have been studied by

**Received:** September 21, 2013

**Revised:** November 17, 2013

**Accepted:** November 25, 2013

**Published:** November 25, 2013

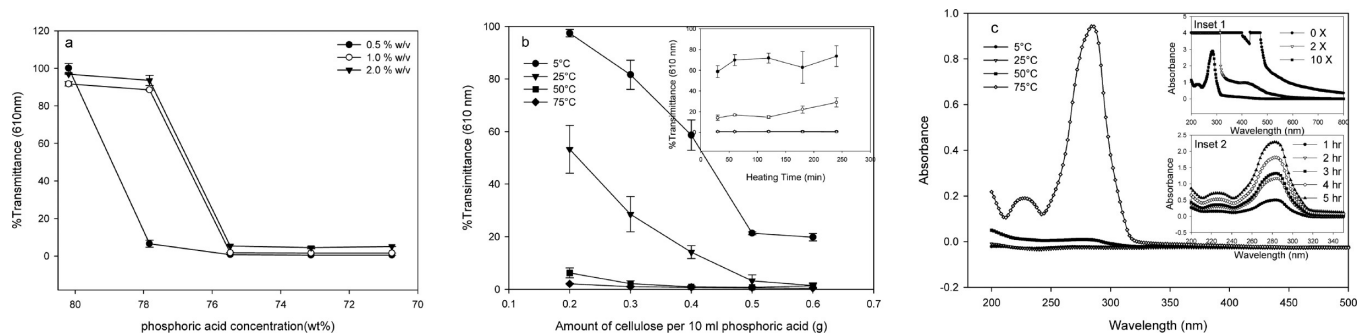


**Figure 1.** Effects of reaction conditions on the dissolution of MCC: (a) effects of phosphoric acid concentration; (b) effects of ratios of MCC/phosphoric acid, incubation temperature, and time (inset); (c) UV-vis spectra of the reaction mixture at different incubation temperatures (incubation time was 30 min and dilution factor was 4); inset 1 of part c is the spectra of the reaction mixture by different dilution factors (incubation temperature was 75 °C and incubation time was 5 h); inset 2 is the spectra of reaction mixture after different incubation time (incubation temperature was 75 °C and dilution factor was 10). Data are represented as mean  $\pm$  standard derivation ( $n = 3$ ).

several researchers.<sup>15–17</sup> Recently, the irreversible adsorption of cellulose nanocrystals at an oil–water interface to stabilize an emulsion by the “Pickering” effect was reported<sup>6,8</sup> and was explained based on the amphiphilic characteristic of cellulose nanocrystals residing in the crystalline organization at the elementary brick level.<sup>6</sup> These studies demonstrated the possibility of using nanocellulose for applications of gelling and emulsion stabilization.

Compared with the extensive research on the crystalline form of cellulose, less research has been devoted to the amorphous form of cellulose. Although it is known that cellulose can be dissolved with solvents including a  $\text{SO}_2$ –diethylamine–dimethylsulfoxide ( $\text{SO}_2$ –DEA–DMSO) solvent system,<sup>18</sup> *N*-methylmorpholine-*N*-oxide,<sup>19</sup> ionic liquid,<sup>20</sup> or alkali/urea aqueous systems<sup>21</sup> and subsequently regenerated with an antisolvent, such as water, ethanol, or acetone, to obtain a mixture of cellulose II and amorphous cellulose, its functional properties remain less thoroughly explored. In this paper, we used a benign solvent—phosphoric acid to dissolve cellulose and characterized the obtained functional material. We have shown by simple disruption of the crystalline structure of cellulose with phosphoric acid that the regenerated cellulose is as versatile as the crystalline form of cellulose in gelling and emulsion stabilization.

## EXPERIMENTAL DETAILS

**Materials.** Dodecane (98%) was purchased from Aladdin (Shanghai, China) and purified by extensive extraction with water. Calcofluor White was purchased from Sigma-Aldrich (Shanghai, China). Original MCC powder (particle size of 20–100  $\mu\text{m}$ ), 85 wt % phosphoric acid ( $\text{H}_3\text{PO}_4$ ), and all other chemicals were purchased from Sinopharm Chemical Reagent Co, Ltd. (Shanghai, China). Deionized water was used throughout the experiment.

**Dissolution and Regeneration of MCC.** Between 0.20 and 0.60 g of original MCC powder was added to a 50 mL centrifuge tube, and then 0.6 mL of deionized water was added to wet the cellulose powder, followed by the addition of 10 mL of precooled or preheated  $\text{H}_3\text{PO}_4$  in aliquots of 4, 4, and 2 mL. The cellulose suspensions were always mixed by a vortex before the addition of  $\text{H}_3\text{PO}_4$  in the next step. In this way, homogeneous cellulose suspensions were obtained and then incubated for durations of up to 5 h. The %transmittances of the cellulose suspensions at 610 nm were measured using a spectrophotometer and used as indexes to show the extent of cellulose dissolution (the higher the %transmittance, the better the dissolution). The effects of  $\text{H}_3\text{PO}_4$  concentration, ratio of cellulose/ $\text{H}_3\text{PO}_4$ , incubation temperature, and time on the dissolution of cellulose were studied in this way. Analysis of the byproduct formation was conducted by

scanning the UV-vis spectra of the incubated cellulose suspensions, directly or after dilution, with a spectrophotometer (LabTech Bluestar A, Beijing, China). Dilution was conducted with deionized water, followed by centrifugation to remove the white cloudy precipitate. A scale-up reaction condition of 5 °C and 24 h with cellulose/water/85 wt % phosphoric acid in a ratio of 1:3:50 (w/v/v) was selected to prepare the regenerated cellulose, followed by repeated centrifugation and dialysis to remove the phosphoric acid until a constant pH was obtained. The purity of the MCC and the yield of the regenerated cellulose were determined by the anthrone method.<sup>22</sup> One-half milliliter of dispersed cellulose was reacted with 4.5 mL of anthrone reagent at 95 °C for 10 min, followed by dilution with anthrone reagent to a proper concentration before reading the absorbance at 620 nm. Three replicates were run for each condition.

**Microscopy.** Optical, fluorescence, and polarized light micrographs of the original MCC and the regenerated cellulose suspensions were captured by an Eclipse microscope equipped with a digital camera (Nikon 80i, Japan). Calcofluor White was used as a fluorescence dye of cellulose at a concentration of 0.1% w/v. Scanning electron microscopy (SEM) of the original MCC powder and freeze-dried regenerated cellulose was performed by an electron microscope (S4800, Hitachi, Japan) at an accelerating voltage of 30 kV. The samples were gold coated in an ion sputter coater for 2 min before observation.

**XRD and FTIR Analysis.** The crystal structures and chemical properties were studied by X-ray diffraction (XRD) and Fourier transform infrared spectroscopy (FTIR). X-ray diffraction (XRD) patterns of the lyophilized samples were collected using an X-ray diffractometer (D8 Advance, Bruker AXS, Germany) equipped with  $\text{Cu K}\alpha$  radiation ( $\lambda = 1.5418 \text{ \AA}$ ) over the range of  $2\theta$  from 8 to 80°. The crystallinity index (CI, %) was determined by eq 1.<sup>23,24</sup>

$$\text{CI (\%)} = 100(I_{\text{Max}} - I_{\text{Am}})/I_{\text{Max}} \quad (1)$$

where  $I_{\text{Max}}$  is the maximum intensity of the principal peak and  $I_{\text{Am}}$  is the intensity of the amorphous cellulose peak at  $2\theta = 18^\circ$ . FTIR spectra of the original MCC and the regenerated cellulose after lyophilization were obtained on a Nicolet 6700 FTIR spectrophotometer using the KBr disk method (sample/KBr ratio, 1/100). The FTIR spectra were recorded over the range of 4000–400  $\text{cm}^{-1}$  with a resolution of 4  $\text{cm}^{-1}$  and 32 total scans.

**Determination of the Phosphorus Content and Degree of Substitution in Regenerated Cellulose.** The content of phosphorus in the lyophilized sample was determined by a Perkin-Elmer Optima 2100 DV inductively coupled plasma optical emission spectrometer (ICP-OES) after microwave digestion with a mixture of nitric acid and hydrogen peroxide. The substitution degree (DS) of phosphorus was calculated by eq 2,

$$\text{DS (\%)} = (m_1/31) \times 100\% / (m_2/162) \quad (2)$$

**Table 1. Purity, Yield, CI, and DS Values of the Original MCC and Regenerated Cellulose<sup>a</sup>**

sample	purity	yield	CI	DS
original MCC	96.4 ± 1.3%		83 ± 3%	0
regenerated cellulose	99.0 ± 0.3%	85.6 ± 1.1%	35 ± 2%	0.0001 ± 0.0001%

<sup>a</sup>Data are represented as mean ± standard derivation ( $n = 3$ ).

where  $m_1$  and  $m_2$  represent the content of phosphorus and the mass of cellulose, respectively; 31 and 162 are the atomic mass of the phosphorus and molecular mass of cellulose monomer units, respectively. Three replicates were run for each testing.

**Stability of Regenerated Cellulose Suspension.** The effects of ionic strength and pH on the stability of the regenerated cellulose suspensions were studied at temperatures of 25 and 50 °C. The suspensions were diluted to 0.6% w/v, and the ionic strengths and pH values were adjusted with solid NaCl, 1 M HCl, or 1 M NaOH, respectively.

**Emulsion Preparation.** The emulsions were prepared by a disperser (T18 digital ULTRA-TURRAX, IKA, Germany) at 10,000 rpm for 3 min using cellulose suspensions as the aqueous phase and purified dodecane as the oil phase in a volume ratio of 9:1. A series of concentrations were diluted from the stock cellulose suspensions at a concentration of 1.6% w/v. Emulsions prepared with the original MCC at the same concentrations were used for comparison.

## RESULTS AND DISCUSSION

**Dissolution and Regeneration of Cellulose.** Phosphoric acid was selected as the solvent to dissolve cellulose. The dissolution mechanism can be described by an esterification reaction: cellulose-OH + H<sub>3</sub>PO<sub>4</sub> → cellulose-O-PO<sub>3</sub>H<sub>2</sub> + H<sub>2</sub>O.<sup>25</sup> When water was used to regenerate cellulose, the reverse reaction occurred: cellulose-O-PO<sub>3</sub>H<sub>2</sub> + H<sub>2</sub>O → cellulose-OH + H<sub>3</sub>PO<sub>4</sub>.<sup>26</sup> Direct dissolution of cellulose in 85% phosphoric acid was difficult because the exterior of the dry cellulose powder dissolved rapidly and formed a viscous layer through which the solvent penetrated very slowly. Prewetting of the cellulose powder was necessary to achieve a quick dissolution, as was reported elsewhere.<sup>25</sup> As shown in Figure 1a, after prewetting, 0.2 g of cellulose was readily dissolved in 10 mL of 85 wt % (final concentration equal to 80.2 wt %) ice-cold phosphoric acid within 30 min. Smaller amounts of cellulose at concentrations of 0.5–1.0% w/v were dissolved in phosphoric acid at a reduced concentration of 77.8 wt %. With further reduction of the phosphoric acid concentration, the solubilization of cellulose was significantly inhibited, as evidenced by the decrease in %transmittance ( $T_{610}$  nm) to 0.77, 1.81, and 5.40 for 2%, 1%, and 0.5% w/v cellulose, respectively (Figure 1a). Zhang et al. showed that ice-cold phosphoric acid (≥83%) dissolved MCC completely, whereas 77 wt % phosphoric acid only caused swelling of the cellulose. In anhydrous phosphoric acid, a liquid crystalline solution containing 38% w/w cellulose could be easily prepared.<sup>27</sup> Thus, the dissolution of cellulose in phosphoric acid depends on the acid concentration and the ratio of cellulose/acid.

The dissolution of cellulose also depended on the reaction temperature, as shown in Figure 1b. With the increase of temperature from 5 to 75 °C, the %transmittance of the cellulose solution decreased at all cellulose/phosphoric acid ratios, revealing a trend of decreasing solubility with increasing temperature. The interaction between water and dry cellulose is strongly exothermic,<sup>28</sup> which may explain this observation. However, reasons such as changes in the structure of water with temperature,<sup>29</sup> the increased contribution of the negative entropy of mixing with increased temperature,<sup>29</sup> or the altered

interaction between cellulose and solvent at low temperature similar to in the cellulose NaOH/urea system cannot be ignored.<sup>30</sup> Further study is needed to investigate the interaction between phosphoric acid and cellulose at low temperature. Nevertheless, the maximum amount of cellulose that can be solubilized by phosphoric acid was limited, even at the lowest temperature. When the concentration of cellulose was increased to 3% w/v, insoluble particles suspended in the solution could be observed with the naked eye and led to a decrease in % transmittance; even a prolonged solubilization time did not improve the extent of solubilization (inset of Figure 1b). In addition to influencing the dissolution process, the temperature had a profound effect on the formation of byproducts. When the cellulose was heated in phosphoric acid at 75 °C for 30 min or at 50 °C for an extended time (≥12 h), the solution turned light brown. The UV-vis analysis of the diluted reaction mixture revealed the presence of a compound with a characteristic absorbance peak at 285 nm (Figure 1c). In the spectrum of the undiluted reaction mixture, a second compound, which was responsible for the light brown color, was identifiable with a characteristic absorbance peak at 450 nm (inset 1 of Figure 1c). The formation of byproducts was intensified at prolonged heating times (inset 2 of Figure 1c). Currently, the chemical structures of these byproducts remain unknown. They are likely associated with the dehydration products of cellulose, such as 5-hydroxymethylfurfural and its polymerized products.<sup>31</sup> Based on these experiments, a scaled-up reaction condition at 5 °C with cellulose/water/85% phosphoric acid in a 1:3:50 ratio was selected for preparing the regenerated cellulose. A heating time of 24 h, instead of 30 min, was selected to ensure that all MCC particles were completely dissolved. Compared with the optimized yield (30%) of the cellulose nanocrystals prepared by hydrochloric acid or sulfuric acid hydrolysis,<sup>10</sup> the yield of our product was remarkably high, consistently reaching 86.6% (Table 1), suggesting that our phosphoric acid treatment is minimally destructive to the cellulose chain, and both the crystalline and amorphous domains are recovered. A recent publication showed that, with phosphoric acid hydrolysis, thermally stable cellulose nanocrystals can be obtained at yields between 76 and 80%.<sup>9</sup> In contrast with this study, our method is based on the dissolution ability of phosphoric acid for cellulose at lower temperature and not the hydrolytic activity at higher temperature.

**Visual and Microscopic Analysis of Regenerated Cellulose.** The 1.6% w/v original MCC suspension was not stable, and sedimentation occurred within a few minutes (Figure 2a). At concentrations higher than 0.6% w/v, the regenerated cellulose formed a homogeneous suspension (Figure 2b), which was stable for at least three months. However, as we discuss later, this stability does not arise from the electrostatic repulsion that stabilizes cellulose nanocrystals whose surfaces are negatively charged. With a further increase in the concentration to 1.6% w/v, an optically opaque gel that resisted flow was obtained (Figure 2c). The optically opaque characteristic suggests that large particles or wide filaments that

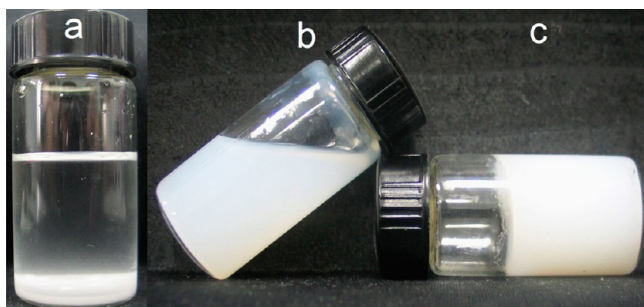


**Figure 2.** Photographs of the 1.6% w/v original MCC suspension (a), 0.6% w/v regenerated cellulose suspension (b), and 1.6% w/v (c) regenerated cellulose gel.

can scatter light are present in the gel. MFC and NFC form a transparent gel because their gel units are so thin that they do not scatter light significantly,<sup>7,11</sup> whereas NCC prepared by sulfuric acid forms a perfectly uniform dispersion in water at low concentrations and self-organizes to a liquid crystal above a critical concentration.<sup>2</sup> Thus, the regenerated cellulose we prepared has a gel-like characteristic similar to that of MFC and NFC. The gel-like characteristic of the regenerated cellulose is also similar to that of partially oxidized dispersed cellulose nanofibers<sup>32</sup> and networked cellulose prepared by the

dissolution of MCC in 70% sulfuric acid and regeneration in ethanol.<sup>33</sup>

The optical, fluorescence, and polarized light micrographs of the original MCC and the regenerated cellulose suspensions were significantly different, as observed by the presence of large crystals only in the former (Figure 3). It is too early to conclude that cellulose loses its crystallinity during the dissolution and regeneration process because the regenerated cellulose crystals may be too small to be observed by a light microscope with a practical resolution limitation of 1  $\mu\text{m}$ . At concentrations higher than 8%, the self-assembly of NCC to form a liquid crystal that displayed birefringence patterns was reported.<sup>17</sup> However, the regenerated cellulose could not be prepared at such a high concentration because of its high viscosity. The SEM analysis revealed the presence of individual large particles in the original MCC (Figure 4a) but not in the regenerated cellulose, where chunky aggregates were observed (Figure 4b and c).

A recent publication has shown that the lyophilization process can induce self-organization of cellulose particles into a lamellar structured foam composed of aligned membrane layers within the concentration range of 0.5 to 1.0 wt %.<sup>34</sup> Therefore, the chunky aggregates in Figure 4b and c were probably also formed by the same lyophilization-induced concentration effect because we use a similar concentration in our lyophilization process. These chunky aggregates were composed of curved, entangled, and aggregated filaments (Figure 4d), which

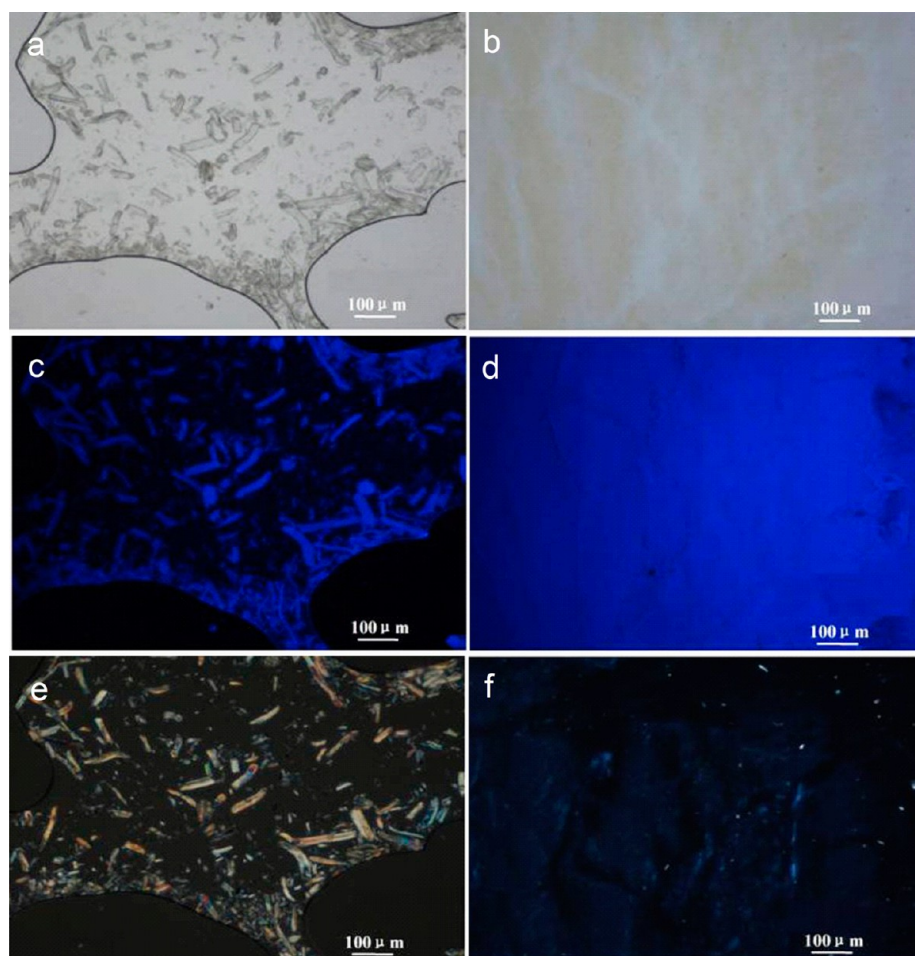


**Figure 3.** Optical (top), fluorescence (middle), and polarized images (bottom) of the original MCC (left) and regenerated cellulose (right). Scale bars: 100  $\mu\text{m}$ .

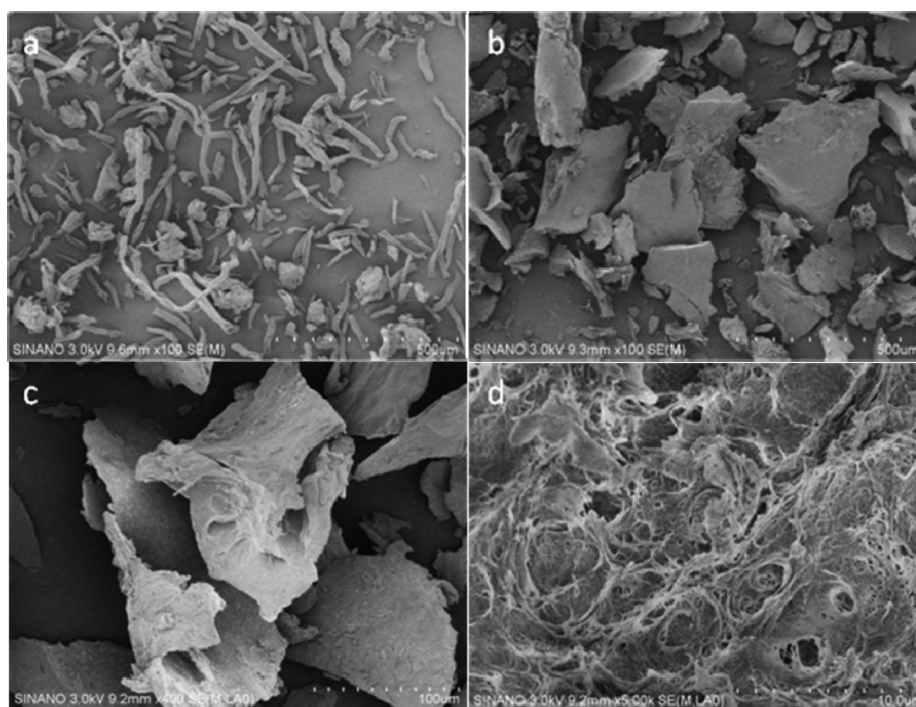


**Figure 4.** SEM images of original MCC (a, scale bar of 500  $\mu\text{m}$ ) and regenerated cellulose (b, scale bar of 500  $\mu\text{m}$ ; c, scale bar of 100  $\mu\text{m}$ ; d, scale bar of 10  $\mu\text{m}$ ).

suggested that the morphology of regenerated cellulose is probably filament-like with a long aspect ratio. Thus, they probably have a high tendency to aggregate during drying.

**X-ray and FTIR Analysis.** The X-ray diffractograms of the original MCC and the regenerated cellulose are shown in Figure 5a. Five peaks were observed for the original MCC at  $2\theta = 14.8^\circ, 16.5^\circ, 20.5^\circ, 22.7^\circ,$  and  $34.6^\circ$ , which correspond to the ( $\bar{1}10$ ), (110), (012), (200), and (004) crystallographic planes of cellulose I, respectively.<sup>12</sup> Compared with the original MCC, less crystallinity was observed for the regenerated cellulose at  $2\theta = 12.3^\circ$  and  $20.3^\circ$ , which correspond to the ( $\bar{1}10$ ) and (110) crystallographic planes of cellulose II.<sup>12</sup> The CI of the regenerated cellulose was calculated to be 35%, which was significantly less than that of the original MCC CI value of 83% (Table 1). In contrast, the cellulose nanocrystals are usually of high crystallinity. Depending on the sources and preparation methods, the CI value can reach 91% for CNC prepared from cotton fibers,<sup>35</sup> 78% from recycled pulp,<sup>36</sup> 81–85% for MCC,<sup>37</sup> and 54–74% for CNC from banana fibers.<sup>38</sup> Although some previous studies showed that treatment of cellulose with concentrated phosphoric acid at 50  $^\circ\text{C}$  led to a mixture of amorphous cellulose, cellulose I, and cellulose II,<sup>39,40</sup> others reported that cellulose regenerated from NaOH/urea and ionic liquid was mainly amorphous with a minor component of cellulose II.<sup>41,42</sup> It was likely that all of the crystalline domains of the cellulose chains were disrupted during the dissolution, whereas some might be realigned and converted to cellulose II during the regeneration and possibly during the drying as well. A similar observation has been made for the dissolution of MCC in 70% sulfuric acid and regeneration in ethanol.<sup>33</sup>

The FTIR spectra of MCC and regenerated cellulose are shown in Figure 5b. The broad bands of the stretching vibrations of the OH groups and  $-\text{CH}_2-$  were observed from 4000 to 2995  $\text{cm}^{-1}$  and at 2900  $\text{cm}^{-1}$ , respectively. The C–O–C bending was from 1170 to 1082  $\text{cm}^{-1}$ , and the C–H

stretching vibration was from 1060 to 1050  $\text{cm}^{-1}$ , all of which match the major functional groups in cellulose.<sup>43,44</sup> The two spectra were similar, proving that the chemical structure of cellulose remained the same after regeneration. There was an O–H bending of absorbed water at approximately 1640  $\text{cm}^{-1}$  in the spectra,<sup>44</sup> which indicated that the water was not completely removed from the cellulose due to the strong interaction of cellulose and water.<sup>34,45</sup> Compared with the spectrum of the original MCC, the peak at 1430  $\text{cm}^{-1}$ , which is attributed to the  $\text{CH}_2$  scissoring motion, disappeared after regeneration, and the relative peak intensity at 895  $\text{cm}^{-1}$ , which is attributed to the C–O–C asymmetric stretching, was increased.<sup>43</sup> The band at 1430  $\text{cm}^{-1}$  is designated as the crystalline absorption band and is more pronounced in cellulose I; the band at 895  $\text{cm}^{-1}$  is designated as the amorphous absorption band and is more pronounced in cellulose II and amorphous cellulose.<sup>46,47</sup> Thus, we can conclude that the cellulose I of the original MCC was converted to amorphous cellulose and cellulose II during regeneration.

Combining the results of XRD, FTIR, and light microscopy, we can draw a firm conclusion that the cellulose lost its crystallinity during the dissolution. During regeneration and probably during drying as well, amorphous cellulose was either partially crystallized into cellulose II, which is more stable than cellulose I,<sup>48</sup> or associated with each other through hydrophobic interactions, which are the driving forces in an amorphous system.<sup>29</sup> This process is depicted by the scheme in Figure 6.

#### Stability of the Regenerated Cellulose Suspension.

The stability of the regenerated cellulose suspension was tested under different conditions by visual observation (Figure 7). With an increase in the ionic strength from 0 to 2 M, an increase in the pH from 1 to 10, and an increase in the temperature from 25 to 50  $^\circ\text{C}$ , the regenerated cellulose was

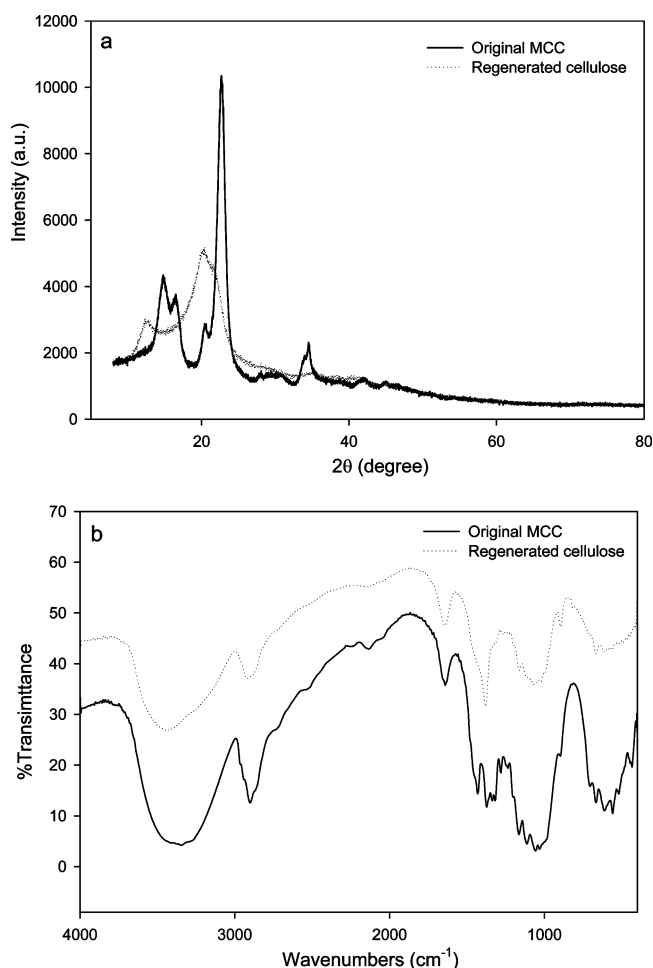


**Figure 5.** XRD (a) and FTIR spectra (b) of original MCC and regenerated cellulose.

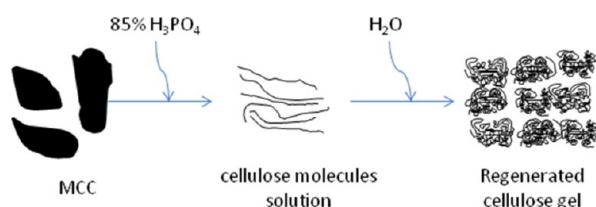


**Figure 6.** Schematic representation of gel formation mechanism of regenerated cellulose.

well-dispersed, and no precipitation was found over three months. NCCs prepared by sulfuric acid hydrolysis present good colloidal stability at low ionic strength ( $\text{Na}^+$ , 1 mM) and in the pH range of 2 to 11 but begin to aggregate at high ionic strength ( $\text{Na}^+$ , 10 mM) and a pH of 12, resulting from the screening of electrostatic repulsion,<sup>5</sup> whereas NCCs prepared by HCl hydrolysis only exhibit good colloidal stability at very low ionic strength.<sup>14</sup> Nanofibrillated cellulose (NFC) prepared by enzymatic pretreatment and mechanical disintegration is not stable at decreasing pH or increasing salt concentration.<sup>11</sup> It is then concluded that regenerated cellulose suspensions are not stabilized by electrostatic repulsion as cellulose nanocrystals are because they are insensitive to the change of electrolytes and pH.

Elementary analysis by ICP-OES also supported this conclusion, as shown by the minimal substitution of phosphate

groups on the regenerated cellulose (Table 1). One possible stabilization mechanism for the regenerated cellulose suspension is the repulsive hydration interaction, which arises whenever water molecules strongly bind to a surface containing hydrophilic groups, such as phosphate and sugar groups.<sup>49</sup> During the dissolution and regeneration, charged impurities, such as hemicellulose, were removed, which was reported in the regeneration process by the ionic liquid, 1-allyl-3-methylimidazolium chloride.<sup>50</sup> The resulting regenerated cellulose is not charged but is probably highly hydrated, so it is not sensitive to electrolytes and pH variation. The temperature usually has little influence on the microstructure of nanocylinder dispersions, although a significant change of the microstructure of the CNC dispersion was observed between 35 and 40 °C.<sup>17</sup> Increasing the temperature usually leads to a weakening of the hydration interactions due to the dehydration of sugar groups. In our study, temperature barely affected the stability of the regenerated cellulose suspension. It is possible that the temperatures we tested were not high enough to cause the destabilization.

**Stabilization of Oil in Water (o/w) Emulsion by Regenerated Cellulose.** The effects of different concentrations of regenerated cellulose on the stabilization of o/w emulsions stored at room temperature are illustrated in Figure 8. In emulsions prepared with the original MCC, both significant oiling-off (formation of a layer of pure oil) and creaming were observed at all concentrations (Figure 8a). In comparison, no oiling-off was observed for emulsions stabilized with regenerated cellulose, even at the lowest concentrations. Oiling-off is usually caused by coalescence, in which two or more emulsion droplets merge together to form a single large droplet.<sup>3</sup> Therefore, the regenerated cellulose is very effective in preventing coalescence. This function may be explained by the amphiphilic characteristic of cellulose, a recent topic of much debate.<sup>29</sup> Previously, cellulose was not considered to be a good stabilizer for emulsions because it is insoluble in water due to the strong intermolecular hydrogen bonds. A recent publication showed that neutral cellulose nanocrystals can effectively stabilize water in oil (w/o) emulsions by irreversibly absorbing at the interface due to the amphiphilic character resulting from the crystalline organization.<sup>6</sup> Another recent publication has shown that ionic liquid regenerated cellulose can stabilize both o/w and w/o emulsions.<sup>51</sup> An earlier report showed that, in a regenerated cellulose chain, the equatorial position of the glucopyranose ring where the hydroxyl bonds are located is hydrophilic, whereas the axial direction where the C–H bonds of the cellulose are located is hydrophobic.<sup>52</sup> Although an earlier publication suggested that the amphiphilic property of cellulose is caused by the presence of a nitrogen-containing impurity,<sup>53</sup> it was unlikely in our study because the original MCC and the amorphous cellulose were of high purity (Table 1).

Nevertheless, our study clearly showed that regenerated cellulose was adsorbed at the interface. This conclusion was drawn from two observations: (1) When low concentration regenerated cellulose was used to stabilize the emulsions, creaming was observed, but the bottom serum phase was clear and free of cellulose (Figure 8b), indicating that oil can attract the cellulose from the water. (2) Fluorescence micrographs demonstrated that regenerated cellulose was adsorbed at the interface (Figure 9a–f). In the fluorescence micrograph, large emulsion droplets with a strong fluorescence surface were observed, demonstrating the adsorption of regenerated

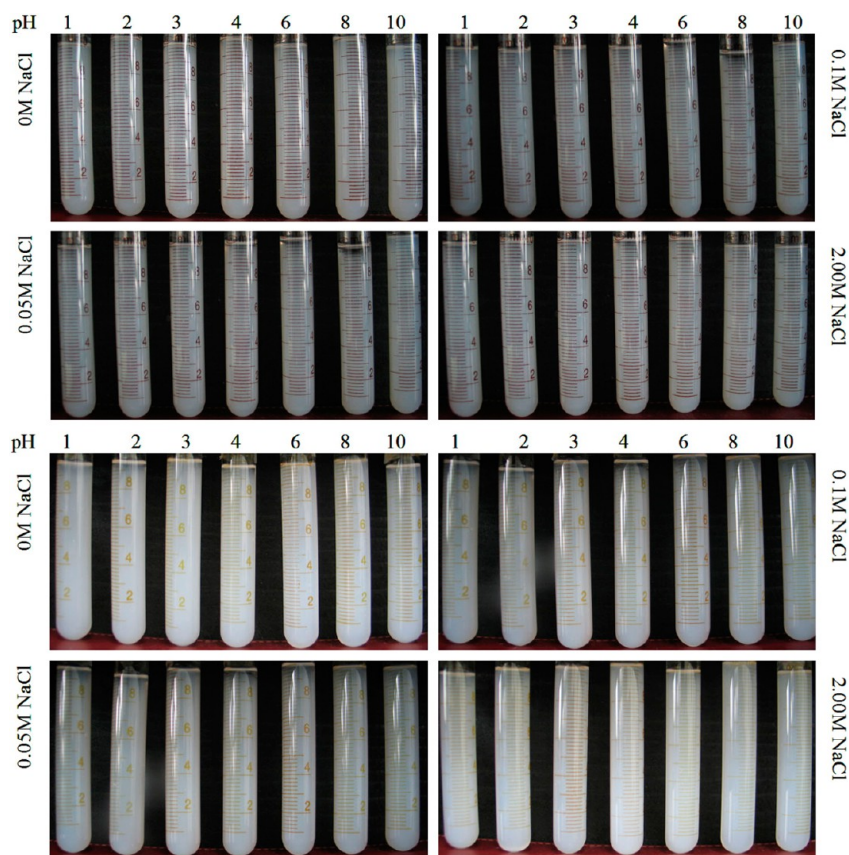


**Figure 7.** Stability of 0.6% w/v regenerated cellulose suspension at different pH values, ionic strengths, and temperatures (graph on top was at 25 °C; bottom was at 50 °C).

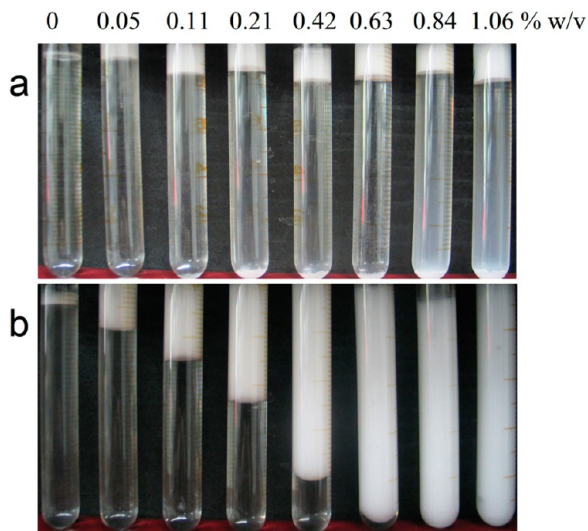


**Figure 8.** o/w emulsions stabilized by the original MCC (a) and the regenerated cellulose (b) at different concentrations: from left to right, the concentrations are 0, 0.05, 0.11, 0.21, 0.42, 0.63, 0.84, and 1.06% w/v; the pictures were taken after 24 h of storage at room temperature.

cellulose at the surface because the fluorescence dye—Calcofluor White—only binds to cellulose. It is arguable that the crystalline portion of the regenerated cellulose was adsorbed at the interface because of the previous report. However, we believe that the amorphous portion might be adsorbed at the interface for two reasons: (1) the same emulsion droplet observed in the optical light micrograph

(Figure 9g) completely disappeared in the polarized micrograph (Figure 9h), indicating that no crystalline cellulose was present in the emulsion system; (2) the crystalline index of the regenerated cellulose was low and was likely caused by the drying process. The real crystallinity in the wet-state was probably much lower. Nevertheless, the adsorption of the regenerated cellulose at the interface was clear.

At the lowest cellulose concentration, the droplet diameter was approximately 61  $\mu\text{m}$ , whereas a stable droplet diameter of 20  $\mu\text{m}$  was observed for all the other concentrations irrespective of the amount of cellulose used (Figure 9a–f). The regenerated cellulose at the concentration 0.11% was enough to cover the surface of the oil droplets to prevent coalescence. A similar observation has been made by a previous report when using neutral cellulose nanocrystals to stabilize emulsions.<sup>8</sup> However, this surface coverage can only prevent coalescence but not creaming. A relatively high concentration of amorphous cellulose, e.g., 0.84%, was needed to prevent creaming. These extra celluloses are used to thicken the aqueous phase and to prevent creaming. Nevertheless, this concentration is much lower than the typical usage of common food polysaccharide-based emulsifiers.<sup>3</sup> Previously, neutral cellulose nanocrystals prepared by the hydrochloric acid hydrolysis of bacterial cellulose were found to stabilize emulsions by the Pickering effect,<sup>8</sup> whereas sulfated nanocrystals did not show interfacial properties.<sup>6</sup> Another author concluded that MFC from mangosteen stabilizes emulsions by forming a solid-like network in the continuous phase, i.e., network stabilization combined with adsorbing at the oil/water interface, Pickering stabilization.<sup>54</sup> Our study also showed that

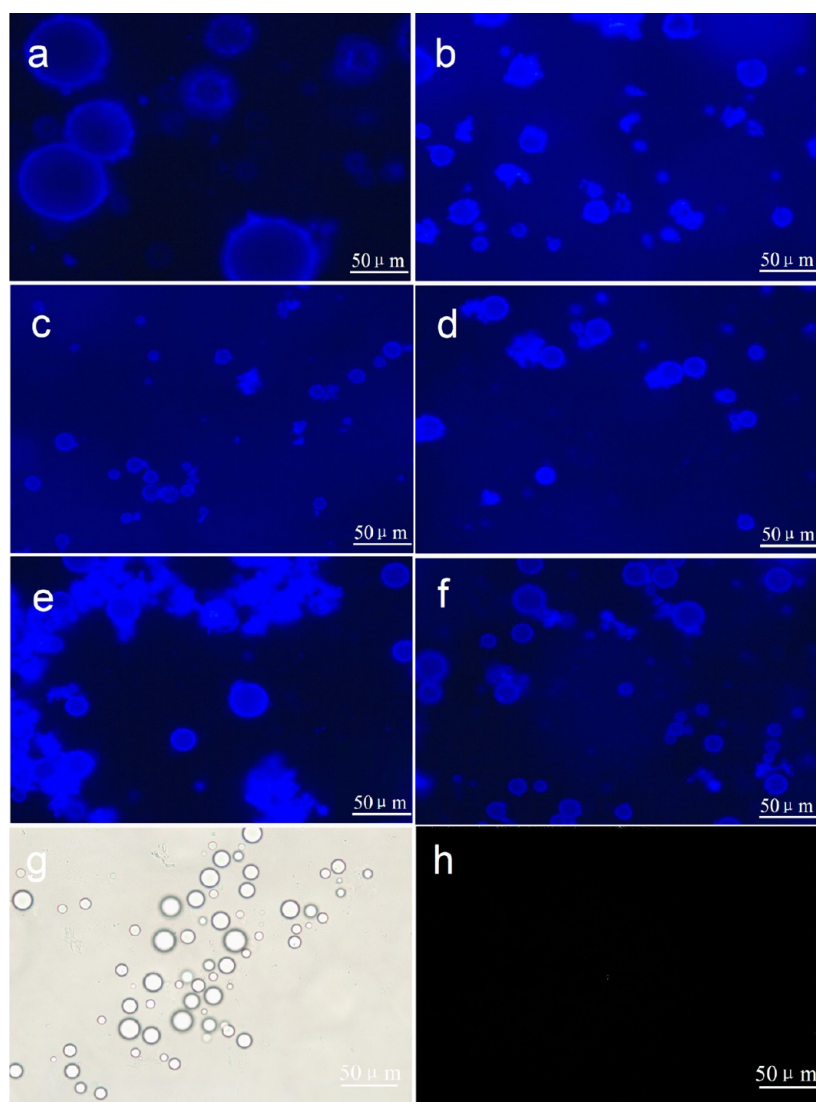


**Figure 9.** Fluorescence (a–f), optical (g), and polarized light (h) micrographs of o/w emulsions stabilized by regenerated cellulose at different concentrations (a–f: 0.05, 0.11, 0.21, 0.42, 0.63, and 1.06% w/v; g–h: 0.21% w/v).

the stabilization mechanism of regenerated cellulose is a combination of network stabilization and Pickering stabilization.

In summary, we described a facile method to produce functional cellulosic material by the dissolution of MCC using cold phosphoric acid followed by regeneration in water. Although phosphoric acid has been used for cellulose decrystallization to improve enzymatic saccharification, it is less frequently used in the preparation of functional cellulose material. Only a very recent publication employed the hydrolytic activity of phosphoric acid at higher temperatures to prepare thermally stable cellulose nanocrystals. Our study used phosphoric acid but relies on its dissolution ability for cellulose at lower temperatures, which has clear benefits over the use of ionic liquid or organic solvents in such a process in terms of availability, cost, and “greenness”. The regenerated cellulose has a morphology and gel characteristics similar to those of MFC and NFC, but it is neutral and is most likely highly hydrated, which makes the resulting suspensions more stable against changes in pH, ionic strength, and temperature. Moreover, the preparation of regenerated cellulose does not consume as much energy as the preparation of MFC and NFC.

Similar to neutral cellulose nanocrystals, the regenerated cellulose can effectively stabilize an oil in water emulsion by adsorption at the interface, which prevents the coalescence and thickening of the aqueous phase, preventing creaming. However, the yield is much higher than that of cellulose nanocrystals whose preparation is based on acid hydrolysis. Compared to the extensive research on crystalline cellulose, the amorphous form cellulose deserves more research input in the future.

#### ■ AUTHOR INFORMATION

##### Corresponding Author

\*Telephone/fax: +86 25 84396907. E-mail address: twu@njau.edu.cn.

##### Notes

The authors declare no competing financial interest.

#### ■ ACKNOWLEDGMENTS

This work is supported by a startup fund (804080) from Nanjing Agricultural University and projects funded by the Priority Academic Program Development of Jiangsu Higher



Education Institutions (PAPD), the General Program of National Natural Science Foundation of China (31271829), and the Natural Science Foundation of Jiangsu Province (BK2012770).

## REFERENCES

- (1) Lima, M. M. D.; Borsali, R. Rodlike cellulose microcrystals: structure, properties, and applications. *Macromol. Rapid Commun.* **2004**, *25*, 771–787.
- (2) Habibi, Y.; Lucia, L. A.; Rojas, O. J. Cellulose nanocrystals: chemistry, self-assembly, and applications. *Chem. Rev.* **2010**, *110*, 3479–3500.
- (3) McClements, D. J. *Food Emulsions: Principles, Practice, and Techniques*, 2nd ed.; CRC Press: New York, 2005; pp 122–146.
- (4) Tuason, D. C.; Krawczyk, G. R.; Buliga, G. Microcrystalline Cellulose. In *Food Stabilisers, Thickeners and Gelling Agents*; Wiley-Blackwell: 2009; pp 218–236.
- (5) Zhong, L. X.; Fu, S. Y.; Peng, X. W.; Zhan, H. Y.; Sun, R. C. Colloidal stability of negatively charged cellulose nanocrystalline in aqueous systems. *Carbohydr. Polym.* **2012**, *90*, 644–649.
- (6) Kalashnikova, I.; Bizot, H.; Cathala, B.; Capron, I. Modulation of cellulose nanocrystals amphiphilic properties to stabilize oil/water interface. *Biomacromolecules* **2012**, *13*, 267–275.
- (7) Klemm, D.; Kramer, F.; Moritz, S.; Lindstrom, T.; Ankerfors, M.; Gray, D.; Dorris, A. Nanocelluloses: a new family of nature-based materials. *Angew. Chem., Int. Ed.* **2011**, *50*, 5438–5466.
- (8) Kalashnikova, I.; Bizot, H.; Cathala, B.; Capron, I. New pickering emulsions stabilized by bacterial cellulose nanocrystals. *Langmuir* **2011**, *27*, 7471–7479.
- (9) Espinosa, S. C.; Kuhnt, T.; Foster, E. J.; Weder, C. Isolation of thermally stable cellulose nanocrystals by phosphoric acid hydrolysis. *Biomacromolecules* **2013**, *14*, 1223–1230.
- (10) Bondeson, D.; Mathew, A.; Oksman, K. Optimization of the isolation of nanocrystals from microcrystalline cellulose by acid hydrolysis. *Cellulose* **2006**, *13*, 171–180.
- (11) Fall, A. B.; Lindstrom, S. B.; Sundman, O.; Odberg, L.; Wagberg, L. Colloidal stability of aqueous nanofibrillated cellulose dispersions. *Langmuir* **2011**, *27*, 11332–11338.
- (12) Sebe, G.; Ham-Pichavant, F.; Ibarboue, E.; Koffi, A. L. C.; Tingaut, P. Supramolecular structure characterization of cellulose II nanowhiskers produced by acid hydrolysis of cellulose I substrates. *Biomacromolecules* **2013**, *13*, 570–578.
- (13) Fras, L.; Laine, J.; Stenius, P.; Stana-Kleinschek, K.; Ribitsch, V.; Dolecek, V. Determination of dissociable groups in natural and regenerated cellulose fibers by different titration methods. *J. Appl. Polym. Sci.* **2004**, *92*, 3186–3195.
- (14) Araki, J.; Wada, M.; Kuga, S.; Okano, T. Flow properties of microcrystalline cellulose suspension prepared by acid treatment of native cellulose. *Colloids Surf., A* **1998**, *142*, 75–82.
- (15) Ishii, D.; Saito, T.; Isogai, A. Viscoelastic evaluation of average length of cellulose nanofibers prepared by TEMPO-mediated oxidation. *Biomacromolecules* **2011**, *12*, 548–550.
- (16) Paakko, M.; Ankerfors, M.; Kosonen, H.; Nykanen, A.; Ahola, S.; Osterberg, M.; Ruokolainen, J.; Laine, J.; Larsson, P. T.; Ikkala, O.; Lindstrom, T. Enzymatic hydrolysis combined with mechanical shearing and high-pressure homogenization for nanoscale cellulose fibrils and strong gels. *Biomacromolecules* **2007**, *8*, 1934–1941.
- (17) Urena-Benavides, E. E.; Ao, G.; Davis, V. A.; Kitchens, C. L. Rheology and Phase Behavior of Lyotropic Cellulose Nanocrystal Suspensions. *Macromolecules* **2011**, *44*, 8990–8998.
- (18) Ciolacu, D.; Ciolacu, F.; Popa, V. I. Amorphous cellulose—structure and characterization. *Cellul. Chem. Technol.* **2011**, *45*, 13–21.
- (19) Fink, H. P.; Weigel, P.; Purz, H. J.; Ganster, J. Structure formation of regenerated cellulose materials from NMMO-solutions. *Prog. Polym. Sci.* **2001**, *26*, 1473–1524.
- (20) Han, J.; Zhou, C.; French, A. D.; Han, G.; Wu, Q. Characterization of cellulose II nanoparticles regenerated from 1-butyl-3-methylimidazolium chloride. *Carbohydr. Polym.* **2013**, *94*, 773–781.
- (21) Liu, S.; Zhang, L. Effects of polymer concentration and coagulation temperature on the properties of regenerated cellulose films prepared from LiOH/urea solution. *Cellulose* **2009**, *16*, 189–198.
- (22) Morris, D. L. Quantitative determination of carbohydrates with Dreywood's anthrone reagent. *Science* **1948**, *107*, 254–255.
- (23) Daud, W. R. W.; Kassim, M. H. M.; Seeni, A. Cellulose phosphate from oil palm biomass as potential biomaterials. *BioResources* **2011**, *6*, 1719–1740.
- (24) Segal, L.; Greely, J. J.; Martin, J. A. E.; Comrad, C. M. An empirical method for estimating the degree of crystalline of native cellulose using the X-ray diffractometer. *Text. Res. J.* **1959**, *29*, 786–794.
- (25) Zhang, Y. H. P.; Cui, J. B.; Lynd, L. R.; Kuang, L. R. A transition from cellulose swelling to cellulose dissolution by o-phosphoric acid: Evidence from enzymatic hydrolysis and supramolecular structure. *Biomacromolecules* **2006**, *7*, 644–648.
- (26) Zhang, J.; Zhang, J.; Lin, L.; Chen, T.; Zhang, J.; Liu, S.; Li, Z.; Ouyang, P. Dissolution of microcrystalline cellulose in phosphoric acid-molecular changes and kinetics. *Molecules* **2009**, *14*, S027–S041.
- (27) Boerstoeel, H.; Maatman, H.; Westerink, J. B.; Koenders, B. M. Liquid crystalline solutions of cellulose in phosphoric acid. *Polymer* **2001**, *42*, 7371–7379.
- (28) Kocherbitov, V. U. S.; Kober, M.; Jarring, K.; Arnebrant, T. Hydration of microcrystalline cellulose and milled cellulose studied by sorption calorimetry. *J. Phys. Chem. B* **2008**, *112*, 3728–3734.
- (29) Glasser, W. G.; Atalla, R. H.; Blackwell, J.; Brown, R. M., Jr.; Burchard, W.; French, A. D.; Klemm, D. O.; Nishiyama, Y. About the structure of cellulose: debating the Lindman hypothesis. *Cellulose* **2012**, *19*, S89–S98.
- (30) Cai, J.; Zhang, L. Rapid dissolution of cellulose in LiOH/Urea and NaOH/Urea aqueous solutions. *Macromol. Biosci.* **2005**, *5*, 539–548.
- (31) Mascal, M.; Nikitin, E. B. Direct, high-yield conversion of cellulose into biofuel. *Angew. Chem., Int. Ed.* **2008**, *47*, 7924–7926.
- (32) Crawford, R. J.; Edler, K. J.; Lindhoud, S.; Scott, J. L.; Unali, G. Formation of shear thinning gels from partially oxidised cellulose nanofibrils. *Green Chem.* **2012**, *14*, 300–303.
- (33) Hashaikeh, R.; Abushammala, H. Acid mediated networked cellulose: preparation and characterization. *Carbohydr. Polym.* **2011**, *83*, 1088–1094.
- (34) Han, J.; Zhou, C.; Wu, Y.; Liu, F.; Wu, Q. Self-assembling behavior of cellulose nanoparticles during freeze-drying: effect of suspension concentration, particle size, crystal structure, and surface charge. *Biomacromolecules* **2013**, *14*, 1529–1540.
- (35) Martins, M. A.; Teixeira, E. M.; Correa, A. C.; Ferreira, M.; Mattoso, L. H. C. Extraction and characterization of cellulose whiskers from commercial cotton fibers. *J. Mater. Sci.* **2011**, *46*, 7858–7864.
- (36) Filson, P. B.; Dawson-Andoh, B. E. Sono-chemical preparation of cellulose nanocrystals from lignocellulose derived materials. *Bioresour. Technol.* **2009**, *100*, 2259–2264.
- (37) Herrera, M. A.; Mathew, A. P.; Oksman, K. Comparison of cellulose nanowhiskers extracted from industrial bio-residue and commercial microcrystalline cellulose. *Mater. Lett.* **2012**, *71*, 28–31.
- (38) Cherian, B. M.; Pothan, L. A.; Nguyen-Chung, T.; Mennig, G.; Kottaisamy, M.; Thomas, S. A novel method for the synthesis of cellulose nanofibril whiskers from banana fibers and characterization. *J. Agric. Food Chem.* **2008**, *56*, 5617–5627.
- (39) Kumar, V.; Kothari, S.; Banker, G. S. Effect of the agitation rate on the generation of low-crystallinity cellulose from phosphoric acid. *J. Appl. Polym. Sci.* **2001**, *82*, 2624–2628.
- (40) Zhang, J.; Zhang, B.; Zhang, J.; Lin, L.; Liu, S.; Ouyang, P. Effect of phosphoric acid pretreatment on enzymatic hydrolysis of microcrystalline cellulose. *Biotechnol. Adv.* **2010**, *28*, 613–619.
- (41) Li, R.; Zhang, L.; Xu, M. Novel regenerated cellulose films prepared by coagulating with water: Structure and properties. *Carbohydr. Polym.* **2012**, *87*, 95–100.

(42) Lan, W.; Liu, C.-F.; Yue, F.-X.; Sun, R.-C.; Kennedy, J. F. Ultrasound-assisted dissolution of cellulose in ionic liquid. *Carbohydr. Polym.* **2011**, *86*, 672–677.

(43) Oh, S. Y.; Yoo, D. I.; Shin, Y.; Seo, G. FTIR analysis of cellulose treated with sodium hydroxide and carbon dioxide. *Carbohydr. Res.* **2005**, *340*, 417–428.

(44) Johar, N.; Ahmad, I.; Dufresne, A. Extraction, preparation and characterization of cellulose fibres and nanocrystals from rice husk. *Ind. Crops Prod.* **2012**, *37*, 93–99.

(45) Moran, J. I.; Alvarez, V. A.; Cyras, V. P.; Vazquez, A. Extraction of cellulose and preparation of nanocellulose from sisal fibers. *Cellulose* **2008**, *15*, 149–159.

(46) Adsul, M.; Soni, S. K.; Bhargava, S. K.; Bansal, V. Facile approach for the dispersion of regenerated cellulose in aqueous system in the form of nanoparticles. *Biomacromolecules* **2012**, *13*, 2890–2895.

(47) Kuo, C.-H.; Lee, C.-K. Enhancement of enzymatic saccharification of cellulose by cellulose dissolution pretreatments. *Carbohydr. Polym.* **2009**, *77*, 41–46.

(48) Isogai, A.; Atalla, R. H. Amorphous celluloses stable in aqueous media. Regeneration from SO<sub>2</sub>-amine solvent systems. *J. Polym. Sci., Part A: Polym. Chem.* **1991**, *29*, 113–119.

(49) Israelachvili, J. N. *Intermolecular and surface forces*, 2nd ed.; Academic Press: New York, 1991; pp 122–133.

(50) Casas, A.; Alonso, M. V.; Oliet, M.; Santos, T. M.; Rodriguez, F. Characterization of cellulose regenerated from solutions of pine and eucalyptus woods in 1-allyl-3-methylimidazolium chloride. *Carbohydr. Polym.* **2013**, *92*, 1946–1952.

(51) Rein, D. M.; Khalfin, R.; Cohen, Y. Cellulose as a novel amphiphilic coating for oil-in-water and water-in-oil dispersions. *J. Colloid Interface Sci.* **2012**, *386*, 456–463.

(52) Yamane, C.; Aoyagi, T.; Ago, M.; Sato, K.; Okajima, K.; Takahashi, T. Two different surface properties of regenerated cellulose due to structural anisotropy. *Polym. J.* **2006**, *38*, 819–826.

(53) Ardizzzone, S.; Dioguardi, F. S.; Quagliotto, P.; Vercelli, B.; Viscardi, G. Microcrystalline cellulose suspensions: effects on the surface tension at the air-water boundary. *Colloids Surf., A* **2001**, *176*, 239–244.

(54) Winuprasith, T.; Suphantharika, M. Microfibrillated cellulose from mangosteen (*Garcinia mangostana* L.) rind: Preparation, characterization, and evaluation as an emulsion stabilizer. *Food Hydrocolloids* **2013**, *32*, 383–394.